

See discussions, stats, and author profiles for this publication at: <https://www.researchgate.net/publication/38072373>

Thermal properties and Brillouin-scattering study of glass, crystal, and "glacial" states in n-butanol

ARTICLE *in* THE JOURNAL OF CHEMICAL PHYSICS · NOVEMBER 2009

Impact Factor: 2.95 · DOI: 10.1063/1.3258645 · Source: PubMed

CITATIONS

24

READS

34

6 AUTHORS, INCLUDING:



R. J. Jiménez Riobóo

Spanish National Research Council

85 PUBLICATIONS 791 CITATIONS

SEE PROFILE



Alexander Krivchikov

B.Verkin Institute for Low Temperature Phy...

73 PUBLICATIONS 476 CITATIONS

SEE PROFILE



Miguel A Ramos

Universidad Autónoma de Madrid

90 PUBLICATIONS 1,615 CITATIONS

SEE PROFILE

Thermal-properties and Brillouin-scattering study of glass, crystal and “glacial” states in *n*-butanol

Merzak Hassaine,¹ Rafael J. Jiménez-Riobóo,² Irina V. Sharapova,³ Oxana A. Korolyuk,³ Alexander I. Krivchikov,³ and Miguel A. Ramos^{1*}

⁽¹⁾*Laboratorio de Bajas Temperaturas, Departamento de Física de la Materia Condensada, C-III, Instituto de Ciencia de Materiales “Nicolás Cabrera”, Universidad Autónoma de Madrid, Cantoblanco, E-28049 Madrid, Spain*

⁽²⁾*Instituto de Ciencia de Materiales de Madrid, Consejo Superior de Investigaciones Científicas (ICMM-CSIC), Cantoblanco, E-28049 Madrid, Spain*

⁽³⁾*B. Verkin Institute for Low Temperature Physics and Engineering of NAS Ukraine, Kharkov 61103, Ukraine*

Abstract

We have investigated through non-commercial calorimetry and elasto-acoustic Brillouin experiments the phase diagram of *n*-butanol, and have measured the specific heat and the thermal conductivity in a wide low-temperature range for its three different states, namely glass, crystal and so-called “*glacial*” states. The main aim of the work was to shed light on the controversial issue of these allegedly *polyamorphic* transitions found in some molecular glass-forming liquids, firstly reported to occur in triphenyl phosphite (TPP) and later in *n*-butanol. Our experimental results show that the obtained “*glacial*” state in *n*-butanol is not an homogenous, amorphous state, but rather a mixture of two different coexisting phases, very likely the (frustrated) crystal phase embedded in a disordered, glassy phase.

*) Corresponding author. Electronic mail: miguel.ramos@uam.es

I. INTRODUCTION

In the last two decades, much attention has been paid to the apparent existence of first-order transitions between two liquid states of a single-component substance or, more generally, between two distinct amorphous states of that substance. This unexpected phenomenon was termed *polyamorphism*,^{1,2} by analogy with the term “polymorphism” referred to solids presenting different crystalline structures. The best known example is probably that of the two amorphous states of water ice³: high-density amorphous (HDA) ice undergoes a first-order phase transition into low-density amorphous (LDA) ice, which is about 23% less dense than the former and with a different arrangement of the local structure. This kind of polyamorphism was later found in other three-dimensional rigid-network systems, such as SiO₂, GeO₂ or Al₂O₃–Y₂O₃.²

The first “polyamorphic” transition for a molecular glass-forming liquid was reported to occur in triphenyl phosphite (TPP) by Kivelson and co-workers.⁴ They observed a new solid phase denoted by them as “glacial” phase, obtained by a first-order, exothermic transformation from the supercooled-liquid state of TPP, either by slowly (~ 0.5 K/min) heating the glass above its glass-transition temperature ($T_g \approx 205$ K) or by an isothermal transformation of the supercooled liquid within the temperature range around 210–230 K. By further heating this “glacial” phase, another first-order transition into the crystal state was observed at about 237 K. If the supercooled liquid was heated much faster instead, it directly crystallized around 240–245 K. All this phenomenology was confirmed by Rössler and co-workers⁵ through further experiments of DSC calorimetry, Brillouin scattering, and dielectric and nuclear magnetic resonance.

The nature and origin of this so-called “glacial” phase remains however controversial. There is even no consensus in the literature whether the “glacial” state is a crystalline or an amorphous structure. Some groups have proposed to explain its origin as a defect-ordered phase within the theory of frustration-limited domains,^{6–8} others as a second amorphous state,² related to the existence of a liquid-liquid transition,^{9–11} and also that it may be a liquid-crystal or a plastic-crystal

state.¹² On the other hand, Hédoux *et al.* have conducted experiments of Raman spectroscopy,¹³ X-ray diffraction,¹⁴ and differential scanning calorimetry (DSC),¹⁵ and have interpreted this transformation process as an aborted crystallization because of a high nucleation rate in a temperature range where the crystal growth is low. Therefore the “glacial” state would be rather a mixture of nanocrystallites and untransformed supercooled liquid.

More recently, the same case of a new solid phase (presumably amorphous) was reported by B.V. Bol’shakov and A. G. Dzhonson¹⁶ in *n*-butanol at ambient pressure, from the analysis of free radical oxidation kinetics: under isothermal conditions in the range 130–160 K, the supercooled liquid transformed gradually into a white or slightly opalescent solid phase. Kurita and Tanaka¹¹ observed the pattern evolution of the supercooled liquid of *n*-butanol to the new “glacial” state during first-order irreversible transformation at around 120 K, applying phase-contrast microscopy, as also they had done with TPP. The transformation of one supercooled liquid to a glassy state of another liquid —with an estimated $T_g=133$ K, around 15–20 K above the conventional glass transition of *n*-butanol— was interpreted as a new evidence of a liquid-liquid transition (hence, of polyamorphism). It has been proposed¹⁰ that a liquid-liquid transition can exist in various molecular liquids which have a tendency to form long-lived locally-favored structures due to the anisotropic interaction.

Again, these interpretations of the “glacial” state as an exotic defect-ordered phase or as a result of a liquid-liquid transition, were contested by Hédoux and co-workers¹⁷ on the basis of Raman-scattering experiments only. They claimed, as in the case of TPP, that the so-called “glacial” phase was nothing else than a mixed crystal-liquid state, not a new amorphous state. With the aim of shedding light on these debated issues, we have investigated through non-commercial calorimetry and elasto-acoustic Brillouin experiments the phase diagram of *n*-butanol, and have measured the specific heat and the thermal conductivity in a wide low-temperature range for its three different states, namely glass, crystal and so-called “glacial” states.

II. EXPERIMENTAL METHODS

A. Materials

High purity samples of *n*-butanol (Aldrich, anhydrous grade, $\geq 99.8\%$ pure, with $<0.005\%$ water and $<0.0005\%$ evaporation residue), also named 1-butanol or *n*-butyl alcohol, were used without further purification. Its molecular weight is 74.12 g/mol.

B. Experimental setup for calorimetry and specific-heat measurements

Both specific-heat measurements and calorimetric studies of the phase diagram of *n*-butanol were conducted by employing a versatile low-temperature calorimetric system, especially designed for glass-forming liquids,^{18,19} that has been described in more detail elsewhere.²⁰ In particular, we have implemented a so-called continuous method that allows accurate heat-capacity determination after coherent cooling and heating runs, using liquid nitrogen as thermal bath. This experimental method somewhat resembles Differential Scanning Calorimetry (DSC) but, contrary to commercial DSC apparatus, it allows direct measurements of the heat capacity based upon simple physical equations, without any *ad hoc* calibrations. Besides, a direct display of the measured dT/dt curves as a function of temperature T , for a constant applied power or also at spontaneous cooling without applying power, provides us with useful thermograms to monitor first-order transitions such as melting and crystallization processes. As an example, Fig. 1a depicts a thermogram with a cooling process of the liquid that vitrifies below 115 K, and a subsequent heating run where glass transition (around $T_g \approx 111$ K) and “*glaciation*” (with an onset around 130 K) features can be observed.

In the present work, a sample amount of 463 mg of *n*-butanol was put into a copper calorimetric cell (of mass 1.293 g), using a clean syringe, then sealing immediately the copper sample-holder to avoid contact with air moisture as much as possible. A check for possible vacuum leaks and corresponding mass losses was performed by exposing the cell to high-vacuum for hours

employing a diffusive pump. A further check on the total mass of the calorimetric cell full of liquid was performed at the end of each period of measurements, showing a very good reproducibility.

C. Experimental setup for thermal-conductivity measurements

The thermal conductivity of different phases of solid *n*-butanol was measured under equilibrium vapor pressure in a experimental setup already described,²¹ using the steady-state potentiometric method. The sample container used was a stainless steel tube 40 mm long and 22 mm in diameter, with a wall thickness of 0.3 mm. The bottom of the container was fixed to the cold zone of the cryostat that is connected to a helium bath. The statistical error in the thermal conductivity coefficient was below 3% for the whole range of measuring temperatures. The total measurement error (~10%) is mainly due to the systematic error in the measurement of geometrical parameters (*e.g.* inner container cross section and spacing between thermometers).

The different states of *n*-butanol were prepared within the container, using different techniques of cooling or heating the same sample, and taking into account the thermal history of *n*-butanol. In short, the glass was prepared by very fast cooling (above 50 K min⁻¹) of the liquid through the glass transition region to the boiling temperature of liquid N₂. Then, helium was used instead as cryogenic liquid, and the thermal conductivity of the glass state of *n*-butanol was measured at gradually decreasing temperature. After reaching the lowest point of the experiment around 2 K, the measurement was continued at increasing temperature up to 120 K. The temporal behavior of the thermal conductivity was then measured at fixed temperature ($T \approx 122$ K). The formation of the “glacial” state caused relaxation (*i.e.* an increase) of the thermal conductivity. Afterwards, the temperature dependence of the thermal conductivity $\kappa(T)$ was measured at the temperature decreasing from 122 K to 2 K. The sample was then heated above the temperature of the transition into the stable crystalline state and held near T_m . The curve $\kappa(T)$ of this stable crystal was then measured from 178 K to 2 K.

D. Experimental setup for Brillouin spectroscopy

High-resolution Brillouin scattering (HRBS) experiments were performed by employing an Ar^+ ion laser ($\lambda_0 = 514.5\text{nm}$) and a Sandercock-type 3+3 tandem Fabry-Pérot interferometer. The experimental setup used at low temperatures for glass-forming liquids such as ethanol has been described in Ref. 22. The volume of liquid butanol introduced in the transparent cuvette was 0.4 ml.

In order to control the quality of the *n*-butanol sample, the refractive index of the liquid at room temperature was determined by using a standard Abbe refractometre obtaining $n_{22.8^\circ\text{C}}^D = 1.3980 \pm 0.0001$. This value confirms the purity of the employed sample. Since no temperature-dependent refractive index and density data of the different states of *n*-butanol were available, only the temperature and time evolution of the backscattering Brillouin frequency shifts will be shown.

III. RESULTS

A. Calorimetry and specific heat

As already shown in Fig. 1a, the conventional glass state of *n*-butanol can be easily obtained by supercooling the liquid below its melting temperature ($T_m = 184\text{ K}$) even at moderate cooling rates, until the glass transition is observed around $T_g \approx 111\text{ K}$ (as measured at heating rates around $+2\text{ K/min}$). When the glass is heated above T_g , the supercooled liquid (SCL) of *n*-butanol undergoes an exothermic process (an apparent first-order transition) into the so-called “glacial” state above 125 K . In our experimental system, the contribution of the sample to the total heat capacity of the calorimetric cell is so important, that an appreciable self-heating effect due to the exothermic process leads to a final temperature well above the initial one, especially if the heating power is not intentionally suppressed by hand.

Once the “glacial” state has been obtained, this remains (meta-) stable, and when further heated above 155 K , it exhibits another exothermic, first-order transition into the stable crystal. This

is illustrated in Fig. 1b, when repeated cooling and heating cycles below the melting point ($T_m = 184$ K) show the stability of the crystal obtained by heating from the “glacial” state. These and other performed thermal cycles of the obtained crystal, by cooling and heating it below $T_m = 184$ K, demonstrate that this is a stable crystalline state indeed, since no further transitions have been then observed.

On the other hand, we have been able to obtain this kind of “glacial” state, either by heating the glass above T_g or also directly by cooling the liquid down to a stabilization temperature, within the temperature range 125–145 K, approximately. In Fig. 2, we show the heating thermograms of several “glacial” states previously obtained at slightly different temperature ranges, by following different thermal protocols. In all cases, the transition of those “glacial” states into the stable crystal begins around 155–160 K, with an exothermic peak at 163–164 K. It is worth mentioning that when we tried to obtain the “glacial” state by employing helium exchange gas to avoid self-heating and stop temperature increase, we always observed curves such as those shown with dashed lines (curves e and f) in Fig. 2. A small feature at around 111 K followed by a exothermic peak at 135–140 K, before the usual crystallization, clearly indicates that by doing so we are interrupting the “*glaciation*” process, leaving a portion of supercooled liquid which becomes a glass. In fact, when it is heated, the corresponding (partial) glass transition at $T_g \approx 111$ K and the end of the “*glaciation*” below 140 K follow, before the whole of the “glacial” state eventually crystallizes then above 155 K, as usual. Comparing their heat capacity curves with that of the glass sample (see inset in Fig. 2), one can estimate that less than 10% of the sample had remained glass in these particular experiments. We observe that the higher the temperature range of the first “*glaciation*” step, the smaller the enthalpy of crystallization thereafter.

Finally, the obtained results for the molar specific heat of the three different states of *n*-butanol (measured at heating rates around +2 K/min) are presented in Fig. 3. The glass transition is observed at $T_g \approx 111$ K, in good agreement with literature.²³ Then, the “glacial” state is obtained by

heating at $T_{\text{glacial}} > 125$ K, and measured from lower temperatures after cooling it. The exothermic crystallization process, discussed above, is observed here as an apparent minimum in the heat capacity at $T > 155$ K. The so-obtained stable crystal does not exhibit any phase transition, when measured in the whole measured temperature range below its melting point at $T_m = 184$ K. We want to remark that specific heats of crystal and “glacial” states are very similar between them, but clearly different from the glass values.

B. Thermal conductivity

The thermal conductivity κ of *n*-butanol was measured for its three low-temperature states (obtained as explained above), and is presented in Fig. 4. As can be observed there, the temperature dependence $\kappa(T)$ of solid butanol is very sensitive to the solid-state structure. The behavior of $\kappa(T)$ for both crystal and “glacial” states clearly differs from that of the glass.

The thermal-conductivity curve of the glass is weakly dependent on temperature in a wide temperature range. The most intense growth of $\kappa(T)$ with temperature is observed at $T < 4$ K. Then, $\kappa(T)$ exhibits the universal plateau of glasses,²⁴ being temperature-independent at $T = 4\text{--}12$ K, followed by a further increase at a rate $d\kappa/dT = 1.5 \cdot 10^{-3} \text{ Wm}^{-1}\text{K}^{-2}$ within $T = 12\text{--}50$ K. At $T > 50$ K, $\kappa(T)$ decreases at increasing temperature at a rate $d\kappa/dT = -0.9 \cdot 10^{-3} \text{ Wm}^{-1}\text{K}^{-2}$. Therefore, $\kappa(T)$ for the glass state of *n*-butanol is very similar to that typically observed for the amorphous structure of other primary alcohols (the curve resembles very much that of 1-propanol).²⁵

On the other hand, the “glacial” state formed from the supercooled liquid of *n*-butanol at $T \approx 122$ K does not exhibit a glass-like $\kappa(T)$, but rather is close to that of a strongly defective crystal. It is also very different from that of the stable crystal, which shows the typical behavior of a molecular crystal.^{25–27} $\kappa(T)$ for the “glacial” state has a smeared phonon maximum near $T = 50$ K. At $2 < T < 20$ K, $\kappa(T)$ grows with temperature roughly as $T^{1.35}$. In the interval $T = 50\text{--}122$ K, $\kappa(T)$ decreases, as in the glass, at the rate $d\kappa/dT = -0.9 \cdot 10^{-3} \text{ Wm}^{-1}\text{K}^{-2}$, and its value is 37% higher than in

the glass. Note that $\kappa(T)$ of the “glacial” state is strikingly lower than that of the glass at $T < 25$ K. The difference decreases sharply with decreasing temperature. This feature is observed in the temperature interval in which phonons propagate in the ballistic regime (the mean free path is much larger than the distance between the nearest molecules).

In the course of the quasi-isothermal transformation of the supercooled liquid into the so-called “glacial” state at $T \approx 122$ K, the thermal conductivity exhibits a prolonged relaxation. The long (over 30 hours) increase in the thermal conductivity is determined by the slow growth of the metastable solid (“glacial”) state whose thermal conductivity (κ_α) is higher than that (κ_L) of the supercooled liquid. When the solid transformation is completed, the resulting “glacial” state remains stable at lower temperatures. As can be seen in the inset of Fig. 4, the relaxation of thermal conductivity is well described by the equation $\kappa(t) = \kappa_L + (\kappa_\alpha - \kappa_L)\rho(t)$, where $\rho(t)$ is the concentration of the new phase. According to the Avrami law, $\rho(t) = [1 - \exp(-t/t_0)^n]$, with $t_0 = 22$ h and $n = 3$.

C. Brillouin spectroscopy

First of all, the virgin *n*-butanol sample was quenched at a rate of 2–3 K/min from room temperature to 90 K. In this way, the glass state of *n*-butanol is readily obtained. The sample was then slowly heated up, in order to follow all the structural transitions until it melts above 184 K. Fig. 5a shows some of those HRBS spectra, taken at different temperatures, on heating that previously obtained glass. Afterwards, the sample was slowly heated to room temperature and left at this temperature for several days. Then the sample was slowly cooled in a continuous way (at 1 hour per spectrum below 187 K) in order to find out if the substance spontaneously crystallized. Fig. 5b shows this evolution of the HRBS spectra on slowly, continuous cooling of the liquid, until a crystallization process is observed at 154 K.

In addition, it was possible to directly observe the optical quality of the sample inside the optical cryostat. The optical quality of the sample changes dramatically when passing from the

supercooled liquid phase (SCL) to the crystalline phase (featured by phonon peaks C1 and C2) in the case of heating (Fig. 5a), as well as in the case of cooling (Fig. 5b). The big increase of the elastic Rayleigh peak is an evidence of this fact. A comparison of the Rayleigh peaks in Fig. 5 indicates that the crystallization process is more dramatic on heating coming from the glassy phase than on cooling coming from the liquid. Moreover, another interesting aspect is the noticeable change in relative intensity between C1 and C2 observed comparing Fig. 5a and Fig. 5b. The crystal phases obtained are of different structural quality. The disappearance of C2 in Fig. 5a could also be due to the huge increase in elastic scattering for the crystalline phase. Also the existence of a low energy mode (LM) is more clearly observed when crystallizing on cooling. The whole temperature-dependent evolution of the HRBS phonon peaks obtained in backscattering geometry is presented in Fig. 6. The temperature behaviour of the longitudinal acoustic phonon has been obtained on heating and starting in the glass phase at 90 K (circles in Fig. 6). It is clear that there are at least four structural transitions in the temperature range investigated. Starting from the lowest temperatures, the first one is the observed transition from the glass phase to the viscous liquid at about 110 K; then, the structural transition from the viscous liquid to a crystalline-like state (presumably, the so-called “glacial” state) at about 132 K; an anomalous temperature dependence of the longitudinal phonon is seen to begin at 156 K, that softens at 174 K; and finally the transition to the liquid at 184 K. On the other hand, when the sample is cooled down slowly from room temperature (diamonds in Fig. 6), only one structural transition is observed in the temperature range $290\text{ K} > T > 130\text{ K}$. An excellent agreement is found between the frequency values in the liquid phase obtained by either heating or cooling. Also the extrapolation of the SCL curve obtained on cooling fits extremely well with the SCL curve obtained on heating from the glass. In both cases there are two phonon peaks (C1 and C2) coexisting for the obtained crystalline phases in the intermediate temperature range.

In order to gain more insight into the nature of the obtained crystalline phases, two additional experiments were performed. The first one was to quench the sample from room temperature to 140 K, to control at that temperature, and to wait until the sample crystallized. The second one was to

quench the sample from room temperature only to 167 K, stabilizing now at that higher temperature, and to wait again until the sample eventually crystallized. In this way, possible differences between crystalline phases could be detected. The main experimental results obtained were the following:

i) The upper graph in Fig. 7 shows HRBS spectra at different temperatures. The spectra at 140 K shows the time evolution of the crystallization process when it has already begun (L and C1 peaks can be seen) and it is fulfilled (C1, C2 and LM peaks can be seen but no more the L peak). The relative intensity of C1 and C2 in these spectra resembles that already observed in Fig. 5a. The low energy mode is important in these spectra, what was not the case in Fig. 5a. The temperature dependence of the backscattering frequency for the different crystalline modes (C1, C2 and LM) is shown in the lower panel of Fig. 7. Until ~ 156 K the temperature behaviour is very flat, then starts changing until ~ 172 K where the frequency begins to drop. This effect is more evident in the case of the frequency associated to C2.

ii) HBRS spectra for different temperatures after crystallization at 167 K are shown in the upper graph of Fig. 8. The spectra were first recorded on cooling from 167 K until 129 K and then on heating up to 188 K, already in the liquid phase. The most striking feature of these spectra is the clear absence of the C1 phonon peak that was always observed in the crystalline phases discussed above. Nor are there any hints about the low energy mode. The temperature dependence of the C2 phonon peak shows no anomalies either on cooling or heating in the temperature range $130 < T < 170$ K and the reproducibility of the experimental data is excellent. A drastic softening for temperatures above 172 K is clearly seen approaching the melting temperature of 184 K. The crystalline phase obtained at 167 K is clearly of a different nature from that obtained at 140 K. While the crystalline phase obtained at 167 K is homogeneous, the one obtained at 140 K seems to be formed by at least two different phases and the relative quantity of each phase is influenced by the way the crystallization was achieved.

IV. DISCUSSION

We have presented a set of complementary calorimetric, thermal and elasto-acoustic experimental data in *n*-butanol, focused on understanding its phase diagram mainly in the 100–200 kelvin range, and especially the very nature of the so-called “glacial” state.

As expected, *n*-butanol is found to be a good glass-former, much better than pure ethanol¹⁸ and almost as good as the two isomers of propanol,^{28–30} which exhibit an even weaker tendency to crystallization. Above the glass-transition temperature $T_g \approx 111$ K, the three kinds of experiments have shown the previously reported “glacial” phase, obtained from the undercooled liquid at temperatures ranging between 122 K and 140 K. At higher temperatures, typically starting above 155 K, this “glacial” state transforms into the stable crystalline state of *n*-butanol, as demonstrated in Fig. 1b. This stable crystalline state can also be obtained by very slowly cooling of the liquid, as exemplified by the Brillouin-scattering experiments of Fig. 5b and especially Fig. 8, and also by additional calorimetric experiments (not shown).

Concerning the most debated intermediate or “glacial” state, all our experiments pointed to the conclusion that it is neither a second amorphous state (we do not see any trace of a second glass transition), nor a distinct (metastable or disordered) crystalline phase, but rather a mixture of nanocrystalline grains and a disordered matrix, either liquid or solid. This mixture state could be likely due to an aborted crystallization process because of a high nucleation rate in a temperature range where the crystal growth is low.^{15,17} As a matter of fact, when we further force to interrupt the “*glaciation*” process by entering helium exchange gas in the internal vacuum chamber at the right moment, a fraction of the sample exhibits a glass-transition feature (at the very same glass-transition temperature of the canonical glass) followed by a smaller exothermic process at 135–140 K, that is the continuation of the interrupted “*glaciation*” process. In any case, all these “mixture phases” exhibit first-order transitions into the stable crystalline state around 160 K.

In addition to those calorimetric evidences, the three employed experimental techniques give further support to the interpretation of the mixed state. As can be deduced from Fig. 2, the higher the temperature range where the “*glaciation*” process has occurred, the smaller the enthalpy ΔH of crystallization is (or, alternatively, the entropy $\Delta S = \Delta H/T_p$, T_p being the temperature of the exothermic peak). This can be simply traced back to a previously larger entropy loss during its corresponding “*glaciation*” step, in turn due to a larger fraction of well-crystallized sample. For example, curve a of Fig. 2 was produced after annealing the heated glass at 125 K for 4 hours, and then the “*glaciation*” proceeded slowly until an effective final temperature of 153 K. (We will define here the initial and final temperatures by the full width at half maximum of the exothermic peak). The entropy variation of this process is determined to be -31.5 ± 1 J/mol·K, and the corresponding later crystallization around 163 K gives -6.2 ± 0.5 J/mol·K. On the other hand, curves b and c obtained by cooling the liquid in a controlled way, and exhibiting final temperatures of “*glaciation*” 3–5 K lower, gave entropy losses of -28 ± 1 J/mol·K and -26.5 ± 1 J/mol·K, respectively, and -7.1 ± 0.4 J/mol·K and -7.7 ± 0.4 J/mol·K for their subsequent crystallizations around 164 K. Curve d gives values almost identical to curve c. It is worth noticing that the entropy losses around 139 K of curves e and f (allegedly, the continuation of the interrupted “*glaciation*”) are -2.0 ± 0.2 J/mol·K and -2.3 ± 0.2 J/mol·K, respectively. Therefore, they are well within the 5–10% range of the typical entropy losses at the “*glaciation*” event, in good agreement with the above-mentioned fact that their specific-heat curves exhibited a glass-transition feature around 5–10% of the full-glass sample.

This calorimetric and thermodynamic picture of the “glacial” state of *n*-butanol (considered as a frustrated, first step into the crystalline state, that is fully achieved after a second step at higher temperatures) resembles very much what Hédoux et al.¹⁵ found in their DSC experiments for TPP. Furthermore, the above observation (see Fig. 3) about the big similarity between the specific heat of

“glacial” and crystal phases, in comparison with that of glass, supports the idea of the “glacial” phase being essentially composed of crystallites of the same nature.

The thermal conductivity measurements performed for the three states of *n*-butanol also support the same view. As can be observed in Fig. 4, the stable crystal presents the typical behavior of a molecular (dielectric) crystal, whereas the glass state exhibits the well-known universal behavior of glasses,²⁴ both qualitatively and quantitatively. On the other hand, the “glacial” state present an unusually low thermal conductivity at low temperatures, incompatible with the universal thermal-conductivity behavior of amorphous solids, and that very likely can be ascribed to a very defective crystal.

Finally, our Brillouin-scattering measurements have also shown the presence of a mixture of elasto-acoustic peaks in the so-called “glacial” state. One of those Brillouin peaks (C2) clearly correspond to the same acoustic peak of the stable crystal state, obtained by isothermal crystallization at 167 K (Fig. 8). Moreover, it is worth noting that this crystalline peak C2 is more intense and better defined, the higher the temperature of the “*glaciation*” process is. The “glacial” state obtained from the liquid at 154 K (Fig. 5b) exhibits C2 peaks stronger than the others, in contrast to those obtained at 132 K from the glass (Fig. 5a) or at 140 K from the liquid (Fig. 7). This is in full agreement with the proposed interpretation, namely that the “*glaciation*” is only a first step of frustrated or aborted crystallization, due to a low crystalline growth rate. This rate increases gradually with temperature, producing less small nanocrystallites (and/or a smaller disordered volume of the sample) with temperature increase. Eventually, above 160 K the substance is able to crystallize completely.

As quoted above, Tanaka *et al.*⁹⁻¹¹ studied in detail the nature of the “glacial” state in TPP and concluded⁹ that the “glacial” states prepared above 216 K contained microcrystallites and thus were certainly inhomogeneous, but those prepared below 215 K did not contain any microcrystallites and thus were the realization of a homogeneous amorphous state corresponding to a second liquid state. Less exhaustive but similar experiments were conducted by Kurita and

Tanaka¹¹ in *n*-butanol. They stated that the “glacial” state obtained after annealing for a few hours the quenched liquid at 115 K, as well as at 128 K, corresponded to a homogeneous (second) liquid state, which exhibited a (second) glass transition at 133 K. In our experiments, we have never observed such a second homogeneous amorphous state, though by annealing the undercooled liquid always at or above 122 K. We also have tried annealing experiments for up to one day at lower temperatures, with the three employed experimental techniques, and no hint of transformation was ever observed. Moreover, Wypych *et al.*¹⁷ conducted isothermal transformations at 120 K of supercooled liquid *n*-butanol, and their Raman-scattering experiments clearly indicated that the produced “glacial” state was indeed a mixed crystallites-supercooled liquid state. They also performed an isothermal transformation at 125 K, its only difference being a faster crystallization kinetics and a higher degree of crystallinity, supporting the abovementioned view that the “glacial” state is the consequence of a frustrated crystallization process, which occurs in a temperature window where the nucleation rate is high but the growth rate is too low.

V. SUMMARY AND CONCLUSION

We have presented complementary experiments and measurements of calorimetry, specific heat, thermal conductivity and Brillouin scattering to explore the phase diagram of *n*-butanol at low temperatures, which was supposed to comprise three different states: glass, crystal and “glacial” states. All our experimental results have shown that the so-called “glacial” state obtained above 120 K in *n*-butanol appears to be a mixture of (submicron-size) grains of the stable crystal coexisting with a disordered phase. We have not found any evidences of polyamorphism in *n*-butanol. The size and ratio of crystalline sample increase with increasing temperature of the “*glaciation*” process of the undercooled liquid. X-ray or neutron diffraction experiments on the three solid phases of *n*-butanol would be most valuable to confirm this view.

ACKNOWLEDGEMENTS

This work was financially supported in part by the Spanish Ministry of Science within project FIS2006-01117, joint projects of NAS of Ukraine and Russian Foundation for Fundamental Research (Agreement N 9-2009, Subject: “Collective processes in metastable molecular solids”) and program CONSOLIDER Nanociencia Molecular CSD2007-00010, as well as by the Comunidad de Madrid through program “Science and Technology in the Millikelvin” (S-0505/ESP/0337).

REFERENCES

- ¹ C. A. Angell, Science **267**, 1924 (1995).
- ² J. Senker and E. Rössler, Chem. Geol. **174**, 143 (2001).
- ³ O. Mishima, L.D. Calvert, E. Whalley, Nature **314**, 76 (1985).
- ⁴ A. Ha, I. Cohen, X. Zhao, M. Lee, and D. Kivelson, *Supercooled Liquids and Polyamorphism*, J. Phys. Chem. **100**, 1 (1996).
- ⁵ J. Wiedersich, A. Kudlik, J. Gottwald, G. Benini, I. Roggatz, and E. Rössler, J. Phys. Chem. B **101**, 5800 (1997).
- ⁶ I. Cohen, A. Ha, X. Zhao, M. Lee, T. Fischer, M. J. Strouse, and D. Kivelson, J. Phys. Chem. **100**, 8518 (1996).
- ⁷ B. G. Demirjian, G. Dosseh, A. Chauty, M. Ferrer, D. Morineau, C. Lawrence, K. Takeda, D. Kivelson, and S. Brown, J. Phys. Chem. B **105**, 2107 (2001).
- ⁸ Ch. Alba-Simionesco and G. Tarjus, Europhys. Lett. **52**, 297 (2000).
- ⁹ H. Tanaka, R. Kurita, and H. Matakai, Phys. Rev. Lett. **92**, 025701 (2004).
- ¹⁰ R. Kurita and H. Tanaka, Science **306**, 845 (2004).
- ¹¹ R. Kurita and H. Tanaka, J. Phys.: Condens. Matter **17**, L293 (2005).
- ¹² G.P. Johari and C. Ferrari, J. Phys. Chem. B **101**, 10191 (1997).
- ¹³ A. Hédoux, Y. Guinet, and M. Descamps, Phys. Rev. B **58**, 31 (1998).
- ¹⁴ A. Hédoux, O. Hernandez, J. Lefèbvre, Y. Guinet, and M. Descamps, Phys. Rev. B **60**, 9390 (1999).
- ¹⁵ A. Hédoux, Y. Guinet, M. Foulon, and M. Descamps, J. Chem. Phys. **116**, 9374 (2002).
- ¹⁶ B.V. Bol'shakov and A.G. Dzhonson, Dokl. Phys. Chem. **393**, 318 (2003); J. Non-Cryst. Solids **351**, 444 (2005).
- ¹⁷ A. Wypych, Y. Guinet, and A. Hédoux, Phys. Rev. B **76**, 144202 (2007).

- ¹⁸ (a) M.A. Ramos, I.M. Shmyt'ko, E.A. Arnautova, R.J. Jiménez-Riobóo, V. Rodríguez-Mora, S. Vieira, and M.J. Capitán, *J. Non-Cryst. Solids* **352**, 4769 (2006); (b) B. Kabtoul, R.J. Jiménez-Riobóo, and M.A. Ramos, *Philosophical Magazine* **88**, 4197 (2008).
- ¹⁹ (a) A. Mandanici, M. Cutroni, A. Triolo, V. Rodríguez-Mora, and M.A. Ramos, *J. Chem. Phys.* **125**, 054514 (2006); (b) A. Triolo, A. Mandanici, O. Russina, V. Rodríguez-Mora, M. Cutroni, C. Hardacre, M. Nieuwenhuyzen, H.J. Bleif, L. Keller, and M.A. Ramos, *J. Phys. Chem B* **110**, 21357 (2006).
- ²⁰ E. Pérez-Enciso and M. A. Ramos, *Termochimica Acta* **461**, 50 (2007).
- ²¹ (a) A. I. Krivchikov, V. G. Manzhelii, O. A. Korolyuk, B. Ya. Gorodilov, and O. O. Romantsova, *Phys. Chem. Chem. Phys.* **7**, 728 (2005); (b) A. I. Krivchikov, B. Ya. Gorodilov, and O. A. Korolyuk, *Instrum. Exp. Tech.* **48**, 417 (2005).
- ²² R. J. Jiménez-Riobóo, B. Kabtoul and M. A. Ramos, *Eur. Phys. J. B* **71**, 41 (2009).
- ²³ Z. Nan and Z.C. Tan, *J. Therm. Anal. Cal.* **87**, 539 (2007).
- ²⁴ R. C. Zeller and R. O. Pohl, *Phys. Rev. B* **4**, 2029 (1971).
- ²⁵ A.I. Krivchikov, A.N. Yushchenko, and O.A. Korolyuk, F.J. Bermejo, R. Fernández-Perea, I. Bustinduy, and M.A. González, *Phys. Rev. B* **77**, 024202 (2008).
- ²⁶ A.I. Krivchikov, A.N. Yushchenko, V.G. Manzhelii, O.A. Korolyuk, F.J. Bermejo, R. Fernández-Perea, C. Cabrillo, and M.A. González, *Phys. Rev. B* **74**, 060201(R) (2006).
- ²⁷ A.I. Krivchikov, A.N. Yushchenko, and O.A. Korolyuk, F.J. Bermejo, C. Cabrillo, and M.A. González, *Phys. Rev. B* **75**, 214204 (2007).
- ²⁸ C. Talón, M. A. Ramos, S. Vieira, I. Shmyt'ko, N. Afonikova, A. Criado, G. Madariaga, and F. J. Bermejo, *J. Non-Cryst. Solids* **287**, 226 (2001).
- ²⁹ C. Talón, F.J. Bermejo, C. Cabrillo, G.J. Cuello, M. A. González, J.W. Richardson, Jr., A. Criado, M.A. Ramos, S. Vieira, F.L. Cumbreira, and L.M. González, *Phys. Rev. Lett.* **88**, 115506 (2002).
- ³⁰ M. A. Ramos, C. Talón, R. Jiménez-Riobóo, and S. Vieira, *J. Phys.: Condens. Matter* **15**, S1007 (2003).

FIGURE CAPTIONS

Fig. 1. (a) Typical thermogram, in absolute dT/dt units, showing the preparation of the metastable “glacial” state: First, a glass is obtained by simply supercooling the liquid. Then, the glass state is heated at a constant applied power through its glass transition $T_g = 111$ K, until the heating process is stopped around 130 K. Then, an irreversible exothermic process supercooled liquid (SCL) \rightarrow “glacial” state occurs. Afterwards, this “glacial” state does not exhibit any feature when is cooled. (b) Thermogram showing a first thermal cycle by heating the “glacial” state of *n*-butanol that exothermically transforms into the crystal state above 155 K. Subsequent and repeated cooling and heating cycles below the melting point ($T_m = 184$ K) show the stability of the obtained crystal state.

Fig. 2. Heating thermograms of several “glacial” states previously obtained following different crystallization histories. Taking the “*glaciation*” temperature range as the full width at half maximum of the exothermic peak, the depicted thermograms correspond to “*glaciation*” at: 138–153 K (a); 137–150 K (b); 138–148 K (c); 139–145 K (d). Dashed curves (e,e') and (f,f') correspond to “*glaciation*” processes interrupted by supplying helium exchange gas. The inset shows that the latter exhibit in their specific-heat curves a glass-transition feature around 5–10% of the total sample.

Fig. 3. Temperature dependence of the specific heat of *n*-butanol for the glass (Δ), “glacial” (∇) and crystal (O) states around the glass-transition temperature region. The glass-transition temperature T_g , the “*glaciation*” transition observed by heating T_{glacial} , and the melting temperature T_m are graphically indicated.

Fig. 4. Temperature dependence of the thermal conductivity of *n*-butanol for the three states: glass (upward triangles), “glacial” (downward triangles) and crystal (circles). Inset: Thermal conductivity variations in the course of supercooled liquid \rightarrow “glacial” state transformation at $T \approx$

122 K. Solid line is the calculation assuming that the volume concentration of the “glacial” state can be described by the Avrami law $\rho(t) = [1 - \exp(t/t_0)^n]$, with $t_0=22$ h, $n=3$.

Fig. 5. (a) HRBS spectra for different temperatures, on heating from the glass at 90 K. At 132 K the liquid phonon peak is still present (L) and two crystalline phonon peaks are clearly seen (C1 and C2). At 144K only the crystalline phonon peaks are observable and C2 is worse defined. At 170 K only a wide C1 peak can be seen. (b) HRBS spectra for different temperatures, on cooling from the liquid state. At 154 K the liquid phonon peak (L) disappeared and three crystalline phonon peaks are clearly seen (C1, C2, and LM for low energy mode). At 140 K only two crystalline phonon peaks are observable (C1 and C2), the LM peak being much worse defined. It is interesting to note the interchange in observed intensities between C1 and C2 peaks with respect to the spectra in (a).

Fig. 6. Brillouin backscattering frequency shift(s) as a function of temperature for the different phases of *n*-butanol. The circles represent the heating run beginning at 90 K from the glass state. The diamonds correspond to the cooling run of the liquid followed by crystallization below 156 K. The different phases correspond to: glass, supercooled liquid (SCL), liquid (L); C1 and C2 are the phonon peaks observed in the crystalline phases (see Fig. 5a,b). The lines mark the temperatures where the different phase transitions or changes take place.

Fig. 7. (a) Temperature HRBS spectra evolution after quenching to, and isothermal crystallization at, 140 K. There are two spectra at 140K taken at different times to observe the crystallization phenomenon before starting the heating run. Again, three crystalline related peaks are observed (C1, C2 and LM) whereas the liquid related peak (L) disappears. Above 170 K, the C2 and LM peaks are much worse defined. (b) Temperature evolution of the crystalline characteristic peaks where slight changes are observed at about 157 K and 172 K, similarly to the findings featured in the heating run of Fig. 6. Note that the relative intensities of C1 and C2 are similar to those in Fig. 5a and opposite to those in Fig. 5b.

Fig. 8. (a) HRBS spectra taken at different temperatures on cooling and on heating after quenching to, and isothermal crystallization at, 167 K. Only one clear peak (C2) is seen in the crystalline phase. The quality of the C2 peak clearly diminishes for temperatures about 170 K and

above. (b) Temperature evolution of the C2 phonon peak on cooling after crystallization (dark circles) and on heating (light squares). No anomalies on cooling are seen. Only above 172 K a clear softening of the C2 phonon peak is observed, similarly to the features reported in Fig. 6 and Fig. 7.

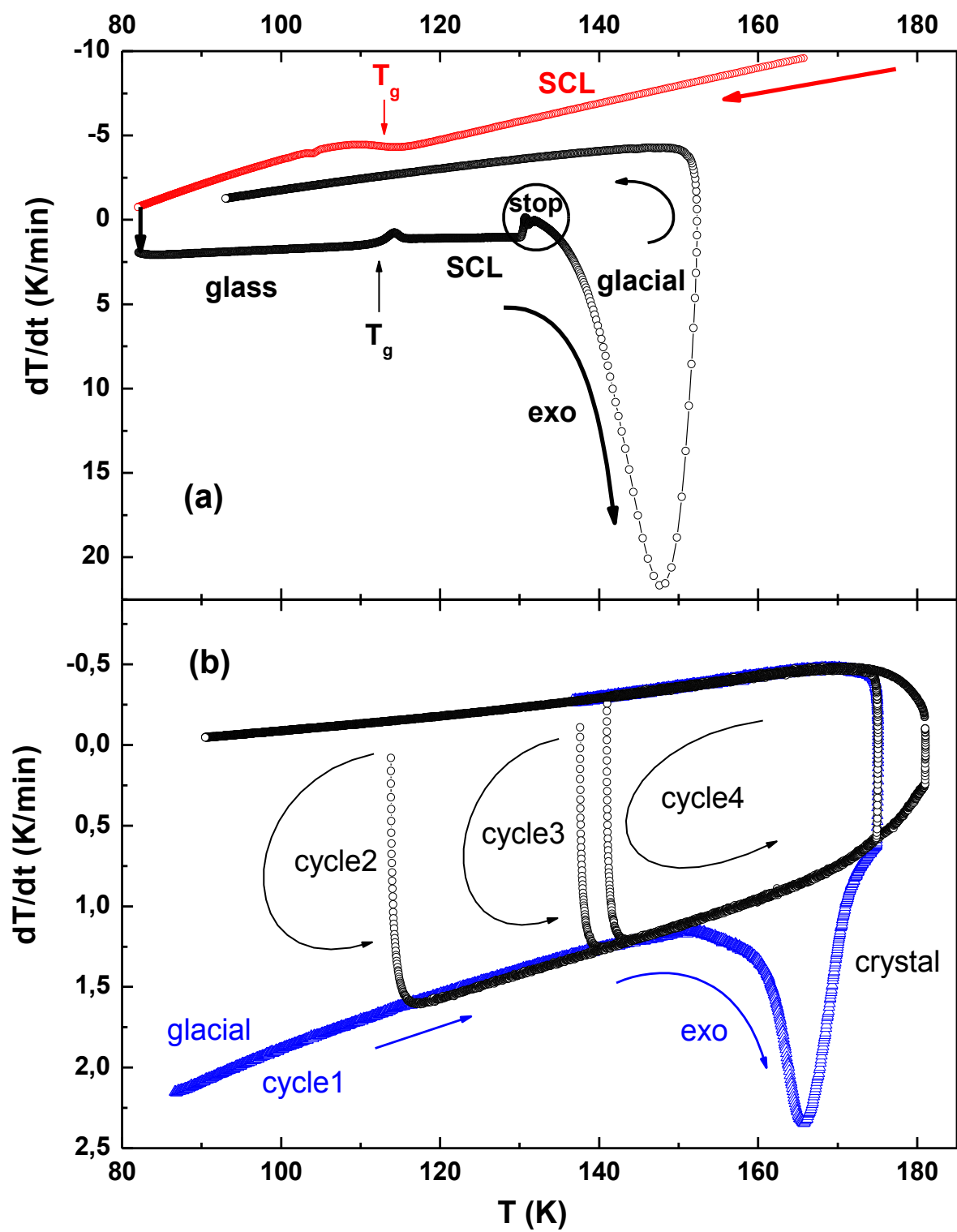


FIGURE 1

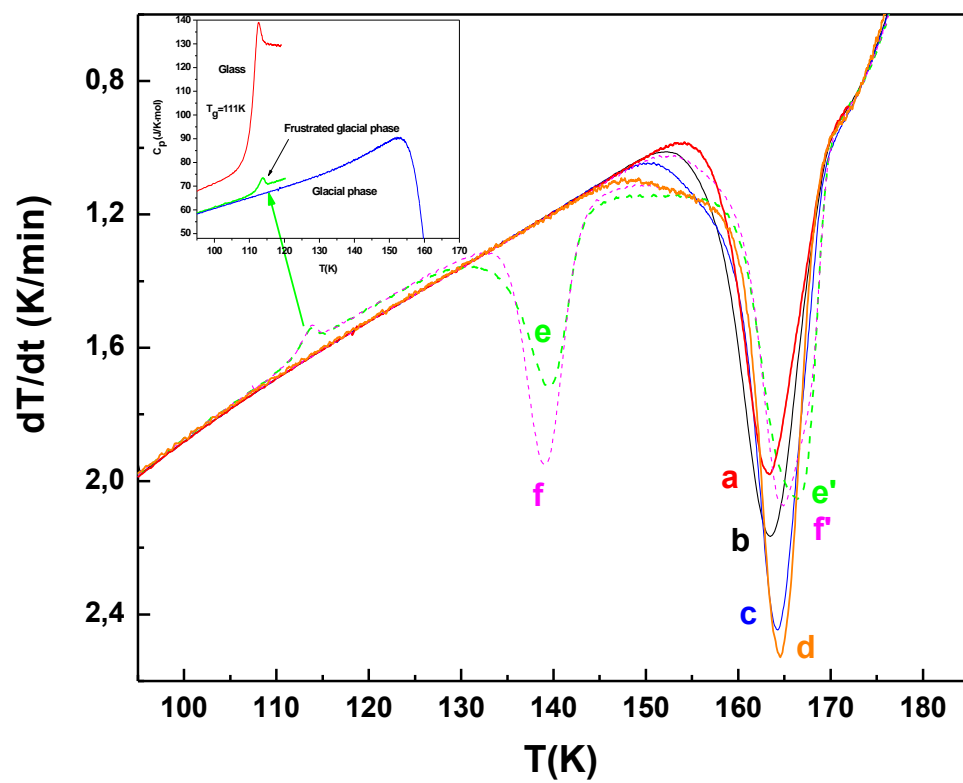


FIGURE 2

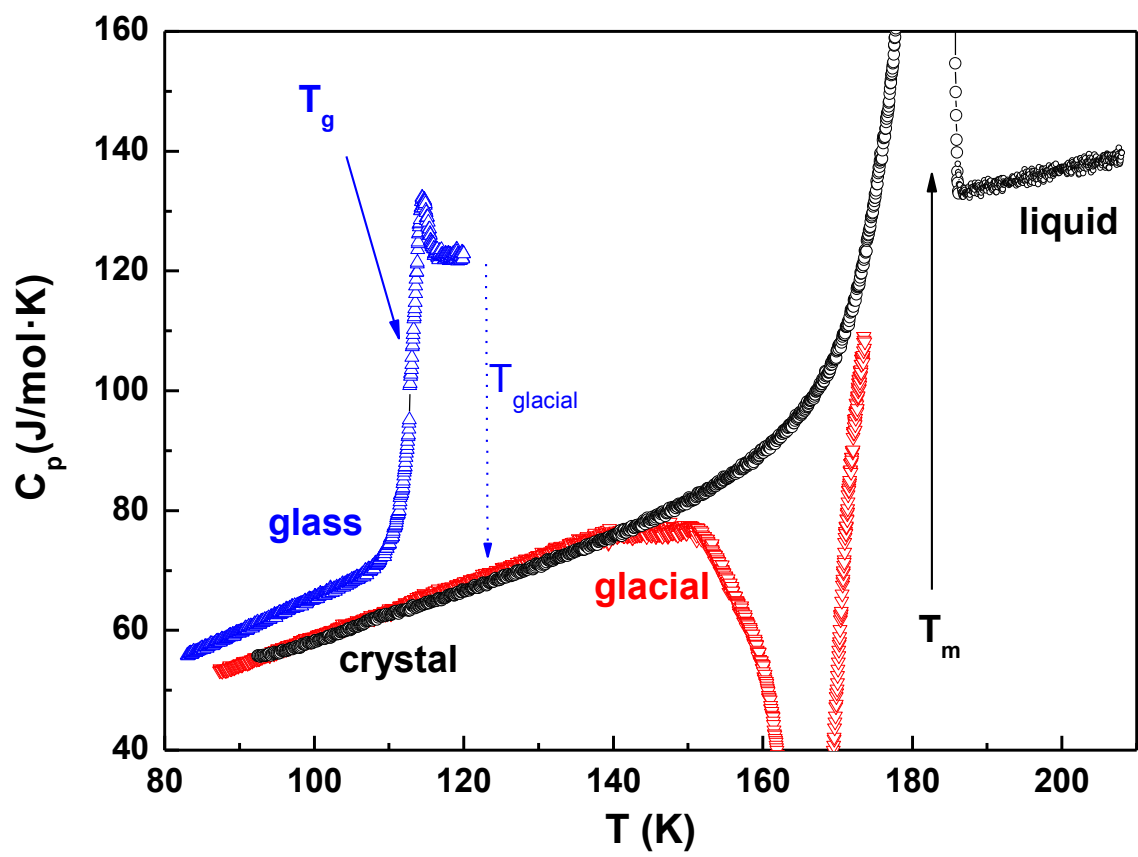


FIGURE 3

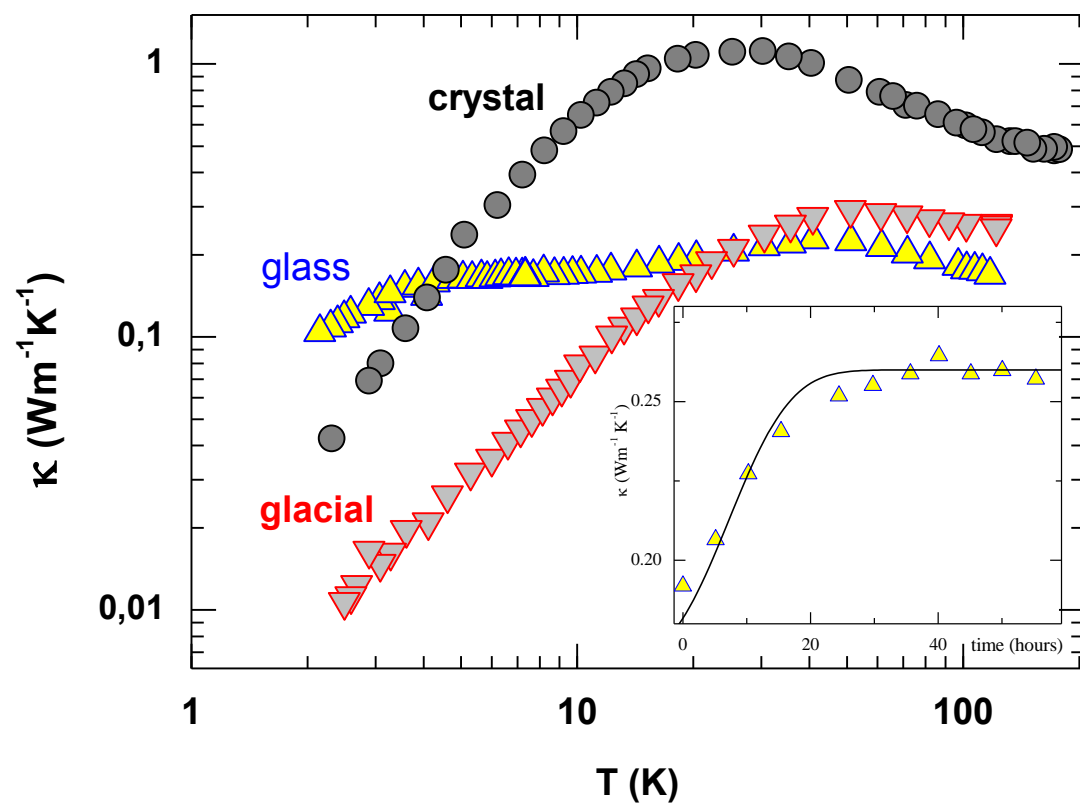


FIGURE 4

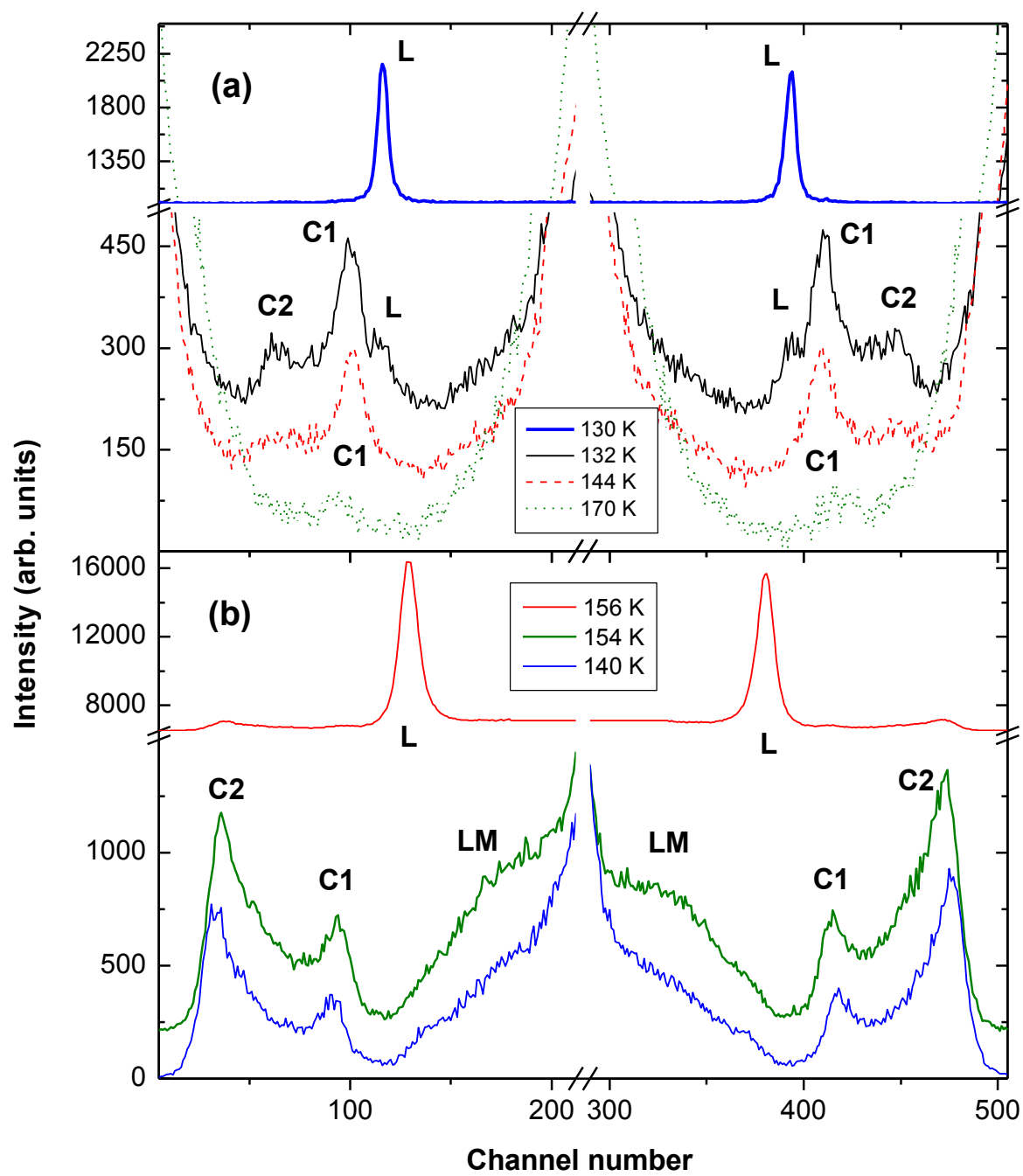


FIGURE 5

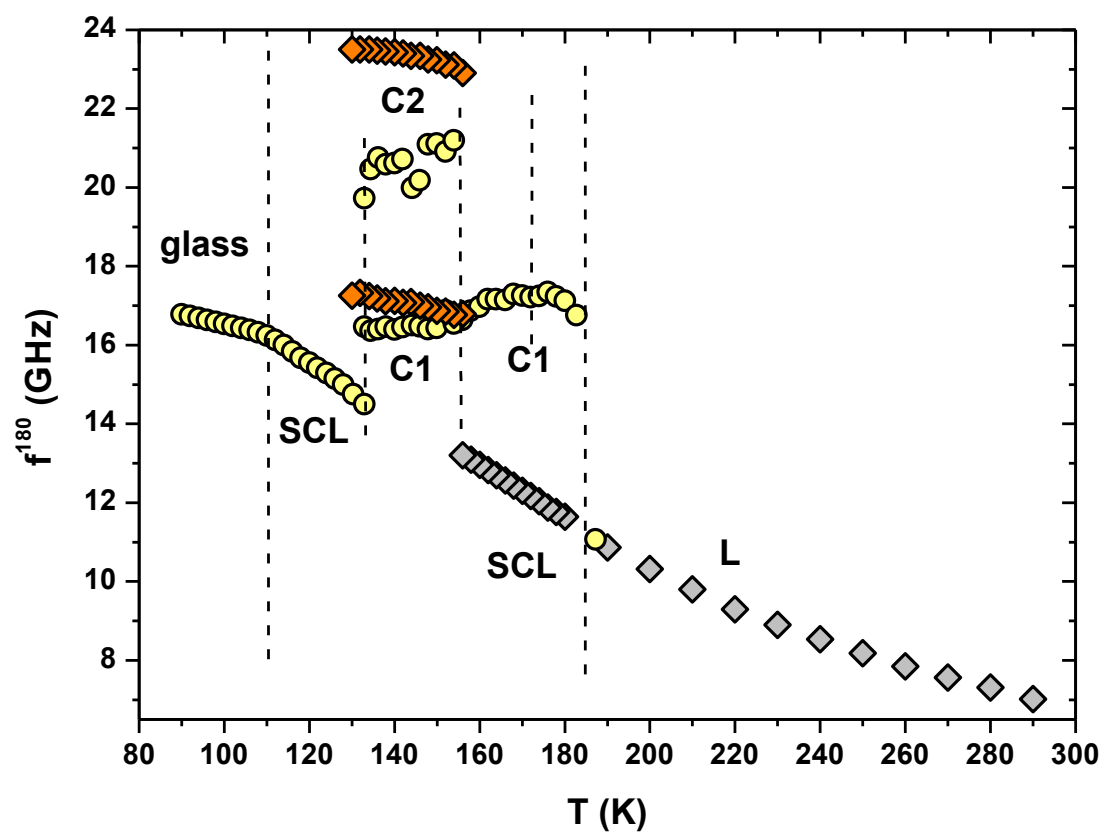


FIGURE 6

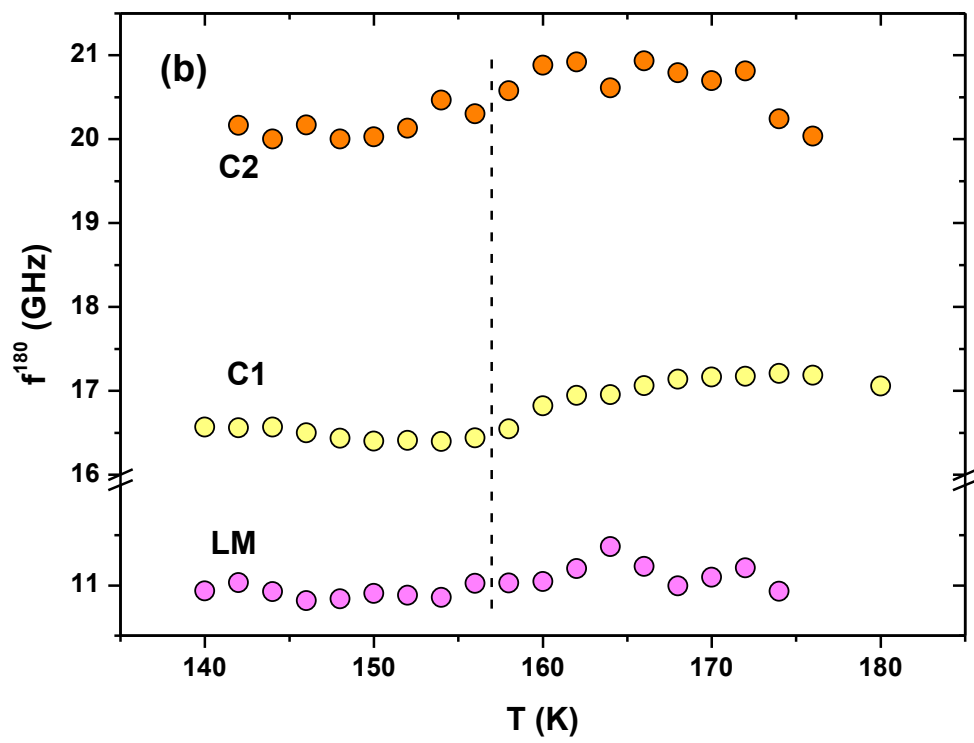
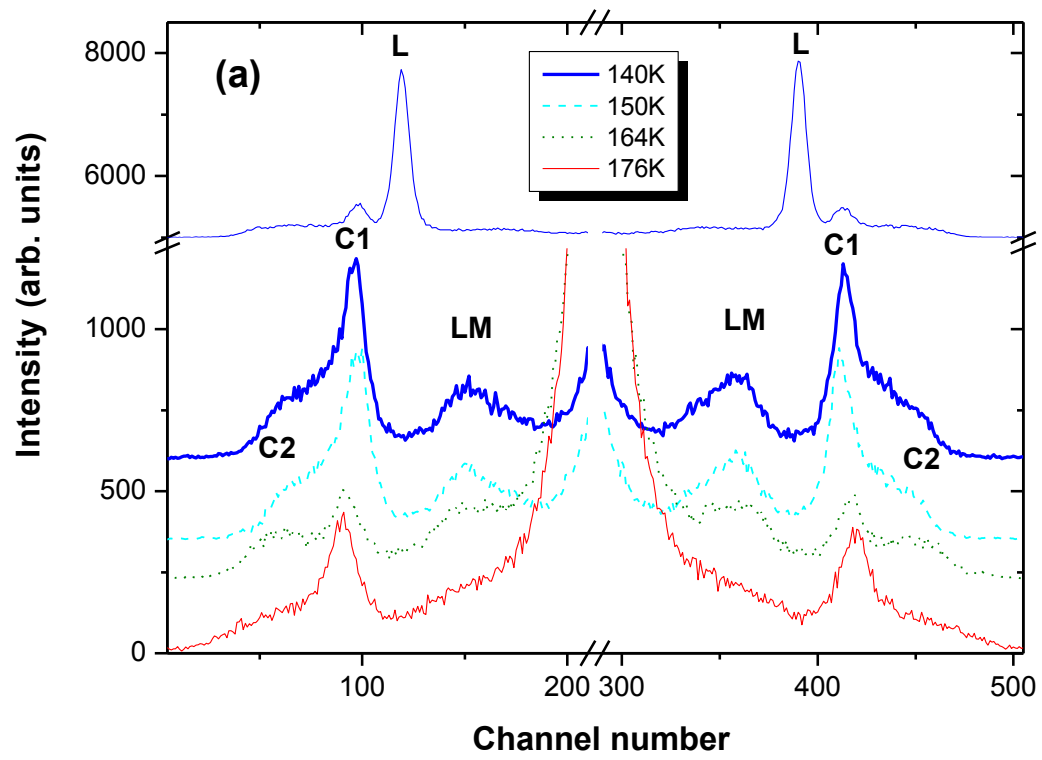


FIGURE 7

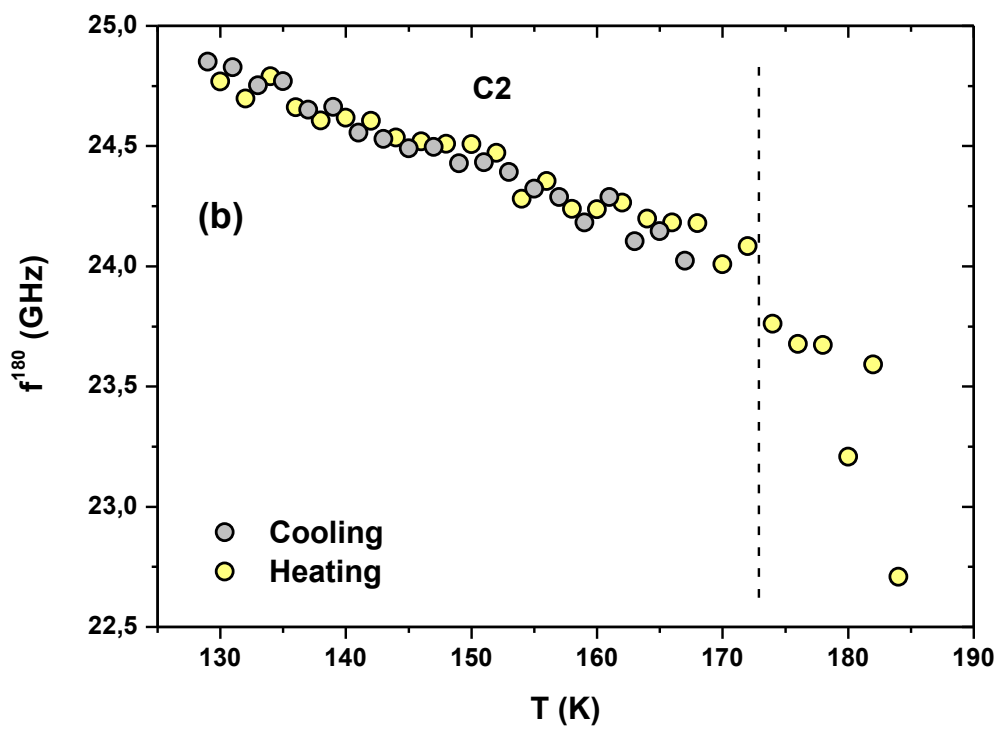
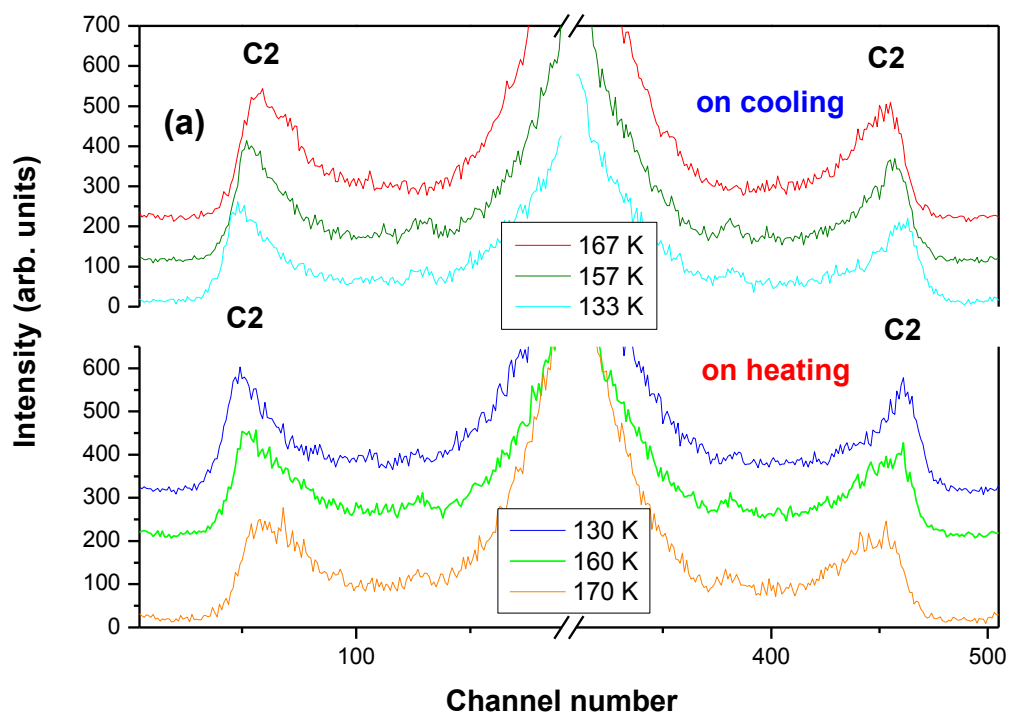


FIGURE 8